Thin spherical shells under rim loading

IIa6

Thin spherical shells under rim loading

Dünne Kugelschalen unter Randbelastung

Paredes delgadas de forma esférica carregadas ao longo do bordo

Voiles minces de forme sphérique chargés le long de leur bord

DR. MILAD M. HANNA,
Ph. D., A. M. I. C. E. – Lecturer, Faculty of Engineering
Abbassia, Cairo

INTRODUCTION

In the analysis of spherical shells of rotational symmetry in loading and support conditions, bending moments and horizontal forces are introduced at the rim to satisfy the boundary conditions. Hence there arises the need for the analysis of spherical shells under these two cases of loading.

The mathematical solution of this problem has already been investigated in previous Papers. (See Bibliography). It involves certain mathematical assumptions and approximations and therefore needs experimental verification. A review of the theoretical analysis is presented in this Paper with the application of the general solution to the conditions of the experimental shells.

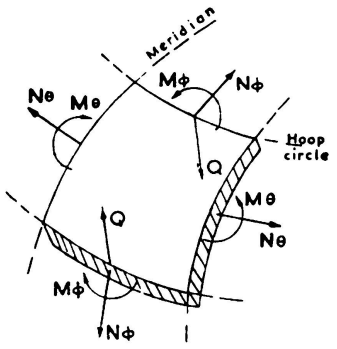

FIG. 1

Figure 1 shows an element of a spherical shell, loaded at the rim only. The position of the element is defined by the angle ψ measured from the rim of the shell (figure 3). For rotational symmetry, the element is loaded only with the forces and moments shown in figure 1, as the element itself is not subjected to external loads. The direct stress components N_Φ and N_ϑ, acting in the meridional and hoop directions respectively are positive when they produce tensile stresses. The bending stress components M_Φ and M_ϑ, acting in the meridional and hoop

directions respectively, are positive when they produce tension on the inner surface of the element.

I. THEORETICAL ANALYSIS

The exact mathematical solution of the problem involves the use of a hypergeometrical series which is slow to converge for thin shells [3] *. The exact solution has therefore become obsolete for design purposes.

Geckeler [1] introduced an approximate solution which is applicable for thin spherical shells with uniform thickness. His solution renders the following equations:

$$
\left.
\begin{aligned}
N_\Phi &= -\cot(\alpha-\psi)\, C\, e^{-\lambda\psi} \sin(\lambda\psi+\gamma) \\
N_\theta &= -\lambda\sqrt{2}\, C\, e^{-\lambda\psi} \sin\left(\lambda\psi+\gamma-\frac{\pi}{4}\right) \\
M_\Phi &= \frac{a}{\lambda\sqrt{2}} C\, e^{-\lambda\psi} \sin\left(\lambda\psi+\gamma+\frac{\pi}{4}\right) \\
M_\theta &= m\, M_\Phi \\
\delta &= -\frac{a}{Eh} \sin(\alpha-\psi)\, \lambda\sqrt{2}\, C\, e^{-\lambda\psi} \sin\left(\lambda\psi+\gamma-\frac{\pi}{4}\right) \\
V &= -\frac{2\lambda^2}{Eh} C\, e^{-\lambda\psi} \cos(\lambda\psi+\gamma)
\end{aligned}
\right\} \quad (1)
$$

where

- δ the horizontal displacement
- V the change of slope of the tangent to the meridian
- a radius of shell
- h thickness of shell
- α half the angle of opening of the shell
- E Young's Modulus
- m Poisson's ratio
- λ the damping coef $= \sqrt{3(1-m^2)}\sqrt{\frac{a}{h}}$

and C & γ are two arbitrary constants to be determined by satisfying the boundary conditions.

Equation (1) defines the stress components in the shell by finding the constants C and γ.

As will be seen later, the experimental shells were provided with horizontal flange rings, as a means of applying the rim loading, as shown in figure 7. This flange ring partially restrained the shell rim in the horizontal direction.

(*) Numbers refer to Bibliography at the end.

Geckeler's solution as given by equation (1), was therefore, applied for the case of rim bending moment under the two limiting boundary conditions: —

a. the rim free to develop the horizontal displacement. This case is referred to as «Theoretical free edge».

b. the rim fully restrained horizontally. This case is referred to as «Theoretical fixed edge».

The case of a shell subjected to rim horizontal force H_α is presented when H_α is applied through a flange ring.

I. Spherical shell subjected to rim bending

a. *Bending Moment Applied to Free Edge*

The boundary conditions for a spherical shell subjected to rim bending moment M_α as show in figure 2, are satisfied by:

$$\left[M_\Phi \right]_{\psi = o} = -M_\alpha \quad \text{and} \quad \left[N\Phi \right]_{\psi = o} = O$$

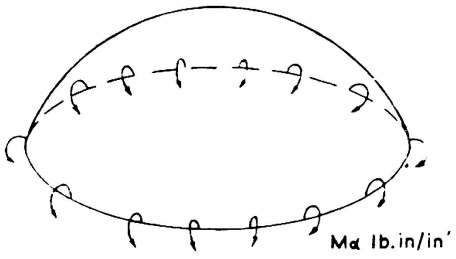

FIG. 2

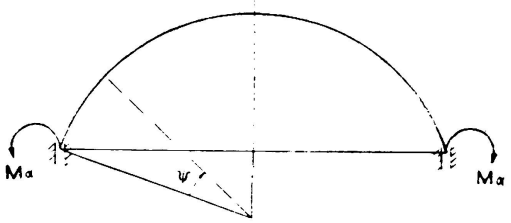

FIG. 3

Substituting in Equation (1), the constants are:

$$\gamma = O \quad \text{and} \quad C = -\frac{2\lambda M_\alpha}{a}$$

Substituting now these constants in Equation (1), the following equations are obtained, giving the stress components for this case:

$$\left.\begin{aligned} N_\Phi &= \frac{2\lambda}{a} M_\alpha \, e^{-\lambda\psi} \sin \lambda\psi \cot (\alpha - \psi) \\ N_\theta &= \frac{2\lambda^2}{a} M_\alpha \, e^{-\lambda\psi} (\sin \lambda\psi - \cos \lambda\psi) \\ M_\Phi &= -M_\alpha \, e^{-\lambda\psi} (\sin \lambda\psi + \cos \lambda\psi) \\ M_\theta &= m \, M_\Phi \end{aligned}\right\} \quad (2)$$

b. *Bending Moment Applied at the Rim when Restrained Horizontally*

This case differs from the previous case a, in that the bending moment is applied to the shell rim when it is fully restrained in the horizontal direction, as shown in figure 3.

The boundary conditions are satisfied for:

$$\left[\ \delta\ \right]_{\psi=o} = O \quad \text{and} \quad \left[\ M_\Phi\ \right]_{\psi=o} = M_\alpha$$

The constants for this case will be:

$$\gamma = \frac{\pi}{4} \quad \text{and} \quad C = -\frac{\lambda\sqrt{2}}{a} M_\alpha$$

Substituting in equation (1), the following equations are obtained:

$$\left.\begin{aligned} N_\Phi &= \frac{\lambda}{a} M_\alpha e^{-\lambda\psi} (\sin\lambda\psi + \cos\lambda\psi) \cot(\alpha - \psi) \\ N_\theta &= \frac{2\lambda^2}{a} M_\alpha e^{-\lambda\psi} \sin\lambda\psi \\ M_\Phi &= -M_\alpha e^{-\lambda\psi} \cos\lambda\psi \\ M_\theta &= m\, M_\Phi \end{aligned}\right\} \quad (3)$$

II. **Spherical shell subjected to rim horizontal force**

a. *Shell with Free Edge*

In a similar manner, the case of a shell subjected to horizontal force H_α, as shown in figure 4, will give the following equation:

$$\left.\begin{aligned} N_\Phi &= -H_\alpha \sin\alpha . e^{-\lambda\psi} (\sin\lambda\psi - \cos\lambda\psi) \cot(\alpha - \psi) \\ N_\theta &= 2 H_\alpha \sin\alpha . e^{-\lambda\psi} \cos\lambda\psi \\ M_\Phi &= \frac{a}{\lambda} H_\alpha \sin\alpha . e^{-\lambda\psi} \sin\lambda\psi \\ M_\theta &= m\, M_\Phi \end{aligned}\right\} \quad (4)$$

b. *Shell with Horizontal Flange*

When the shell is subjected to rim horizontal force H_α applied to flange ring as shown in figure 5a, the force acting at the rim of the shell H'_α (fig. 5b) is given by the equation:

$$H'_\alpha = \frac{ha}{2\lambda b\ h_r + ha} H_\alpha \qquad (5)$$

where b and h_r are the breadth and thickness of the flange ring.

This equation is arrived at by closing the horizontal «gap» between the flange ring and shell as illustrated in figure 5.

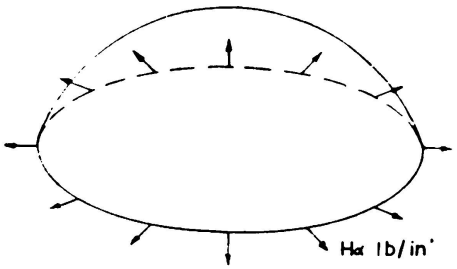

FIG. 4

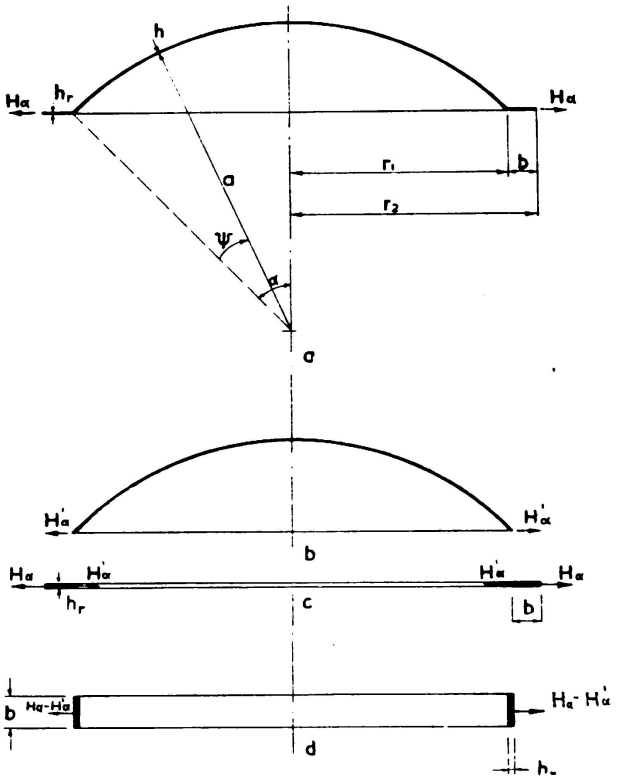

FIG. 5

The edge zone

The mathematical analysis, shows that for both the two cases of rim loading, the forces N_Φ and N_θ and the bending moments M_Φ and M_θ are functions of one of the expressions: —

$1 - e^{-\lambda\psi} \sin \lambda\psi$

$2 - e^{-\lambda\psi} \cos \lambda\psi$

$3 - e^{-\lambda\psi} (\sin \lambda\psi + \cos \lambda\psi)$

$4 - e^{-\lambda\psi} (\sin \lambda\psi + \cos \lambda\psi)$

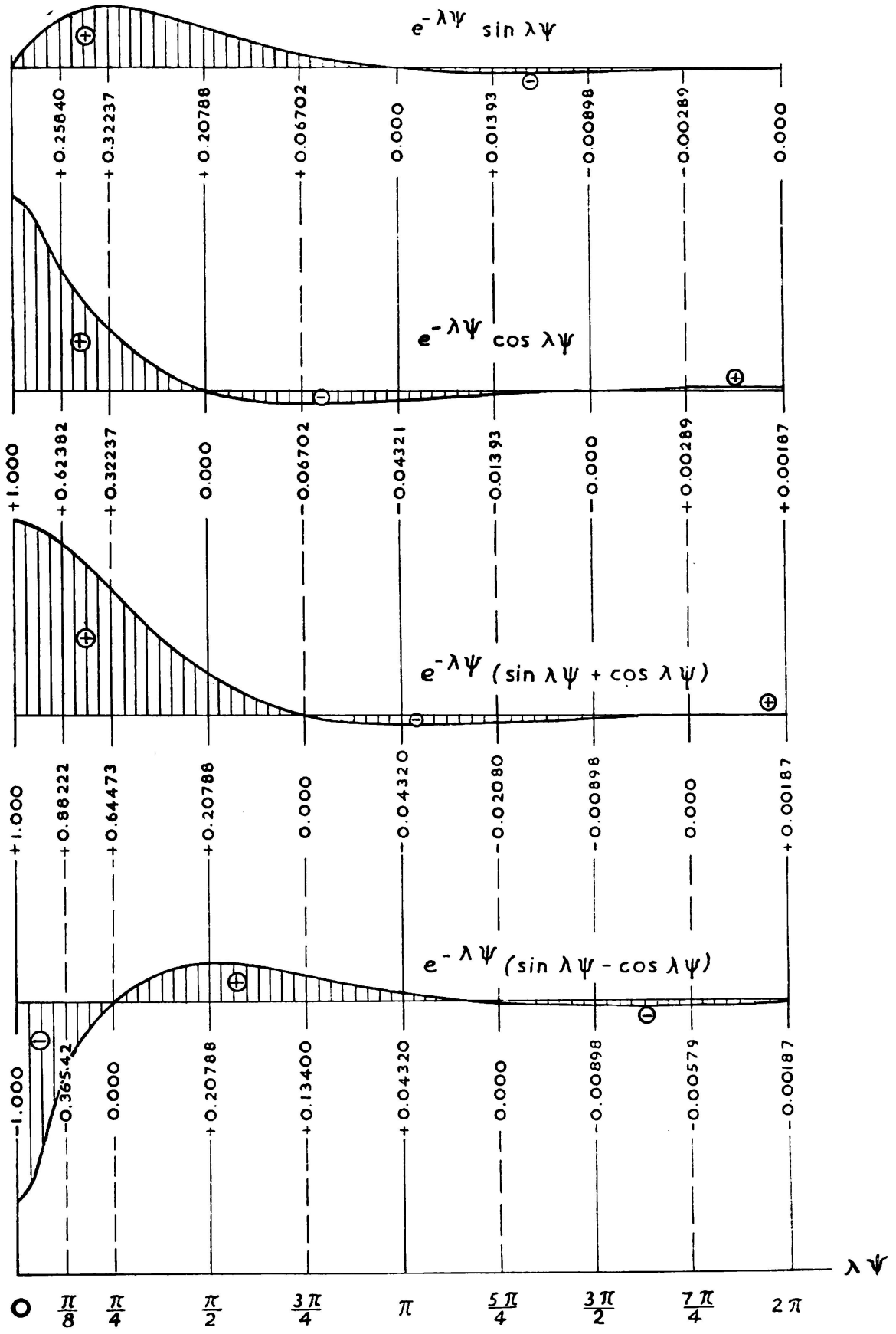
$e^{-\lambda\psi}\sin\lambda\psi$
+0.25840
+0.32237
+0.20788
+0.06702
0.000
+0.01393
-0.00898
-0.00289
0.000
$e^{-\lambda\psi}\cos\lambda\psi$
+1.000
+0.62382
+0.32237
0.000
-0.06702
-0.04321
-0.01393
-0.000
+0.00289
+0.00187
$e^{-\lambda\psi}(\sin\lambda\psi+\cos\lambda\psi)$
+1.000
+0.88222
+0.64473
+0.20788
0.000
-0.04320
-0.02080
-0.00898
0.000
+0.00187
$e^{-\lambda\psi}(\sin\lambda\psi-\cos\lambda\psi)$
-1.000
-0.36542
0.000
+0.20788
+0.13400
+0.04320
0.000
-0.00898
-0.00579
-0.00187
$\lambda\psi$
0
$\frac{\pi}{8}$
$\frac{\pi}{4}$
$\frac{\pi}{2}$
$\frac{3\pi}{4}$
π
$\frac{5\pi}{4}$
$\frac{3\pi}{2}$
$\frac{7\pi}{4}$
2π

FIG. 6

These functions are shown in figure 6. It is clear from the figure that these functions damp quickly and at $\lambda\psi = \pi$ the value of any of these functions is not more than 4.32 % of its maximum value. It is therefore concluded that the effect of the rim loading is mainly confined to the zone defined by the equation $\lambda\psi = \pi$.

If S denotes the width of this edge zone, then,

$$S = a\psi = a\frac{\pi}{\lambda}$$

for Poisson's ratio m = 0.30

$$\lambda = 1.285\sqrt{\frac{a}{h}} \quad \text{and} \quad S = 2.45\sqrt{ah}$$

and for m = 0

$$\lambda = 1.317\sqrt{\frac{a}{h}} \quad \text{and} \quad S = 2.39\sqrt{ah}$$

As will be seen later, the experiments showed that S may be given by the equation:

$$S = 2.0\sqrt{a.h} \tag{6}$$

Spherical shells with variable thickness

The method suggested by Geckeler in dealing with this problem was to divide the shell into several zones by hoop circles. For each zone an average value of λ is used. Starting with the first zone at the edge, the boundary conditions are known and thus the constants C and γ can be determined from equation (1). The stresses components can, now, be calculated at the upper rim of this zone. These values are taken as the boundary conditions for the second zone. Thus again, in equation (1) the boundary conditions are satisfied and new constants are found for the second zone and so on.

Equation (2) for the case of bending moment applied to free rim will give:

$$\left.\begin{aligned} N_\Phi &= \frac{2\lambda}{a} M_\alpha e^{-\Sigma\lambda\psi} \sin \Sigma\lambda\psi \cot(\alpha - \Sigma\psi) \\ N_\theta &= \frac{2\lambda^2}{a} M_\alpha e^{-\Sigma\lambda\psi} (\sin \Sigma\lambda\psi - \cos \Sigma\lambda\psi) \\ M_\Phi &= -M_\alpha e^{-\Sigma\lambda\psi} (\sin \Sigma\lambda\psi + \cos \Sigma\lambda\psi) \\ M_\theta &= m M_\Phi \end{aligned}\right\} \tag{7}$$

Equations (3) and (4) may be modified in a similar manner.

The value of λ that appears as a common factor in any of these equations, is taken as the average of the values for the zone considered and the zones that preceed.

But, as the mathematical solution of equation (1) is based on approximation and as the zone affected by rim loading is very limited, it is thought that if the shell is considered having uniform thickness h at $\lambda\psi = \frac{\pi}{4}$, the curves of distribution would not alter much. In this case, the stress components N_Φ, N_θ and M_Φ may be calculated at $\lambda\psi = \frac{\pi}{8}, \frac{\pi}{4}, \frac{\pi}{2}, \frac{3\pi}{4}$ and π using the coefficient given in figure 6 instead of calculating them at specific values of $\psi°$.

II. EXPERIMENTAL ANALYSIS

The Shell Models

Five aluminium spherical shells were specially constructed for the experiments by A. P. V. Co. Ltd., London. The material had a modulus of elasticity of 10,500,000 lb./sq. in and Poisson's ratio of 0.29.

The shells were shaped by spinning aluminium sheets of uniform thickness on a spherical template 18 inches radius. The process of spinning resulted in a variation of the thickness in the meridional direction. The thickness of the shell was uniform on the same hoop circle. Table I gives the thicknesses of the experimental shells. Each of the five shells will be referred to by the thickness of the plate from which the shell was spun and half the central angle of opening α. For instance the shell ($^1/_4$", 55°) refers to that having an angle of opening 110° and was spun out of a plate $^1/_4$" thick. The five experimental shells were: shell ($^1/_4$", 55°) refers to that having an angle of opening of 110° and was spun out of a plate ($^1/_4$" thick. The five experimental shelle were: ($^1/_4$", 55°), ($^1/_8$", 55°), ($^1/_{16}$", 55°) and ($^1/_8$", 35°), ($^1/_{16}$", 35°).

A rim flange ring was spun monolithically with the shell as shown in figure 7 to provide a means of applying the rim loading. It was desired at the beginning to have the shells with uniform thickness and connected to the rim in a sharp connection as shown in figure 7a. It was only possible to spin the shell with the flange ring by introducing a fillet $^1/_8$" radius between the shell and the flange ring as shown in figure 7b.

The Strain Gauges

Electrical wire resistance strain gauges having a gauge length of 6 millimetres, were fixed at stations corresponding to integral values of $\psi°$. At each station two gauges were fixed on the outer surface, one in the meridional direction and the other in the circumferential direction and similarly two gauges on the inner surface. The gauges were not spaced uniformly on the shell surface. More gauges were fixed at the rim zone

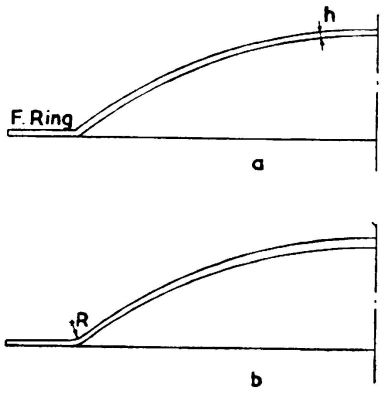

FIG. 7

of the shell to study the stress distribution due to edge loading. At the station corresponding to $\psi = 0°$, i. e., on the fillet between the shell and the flange ring, gauges were fixed on the outer surface, but no gauges could be fixed on the inner surface.

TABLE I

Thicknesses of Experimental Shells

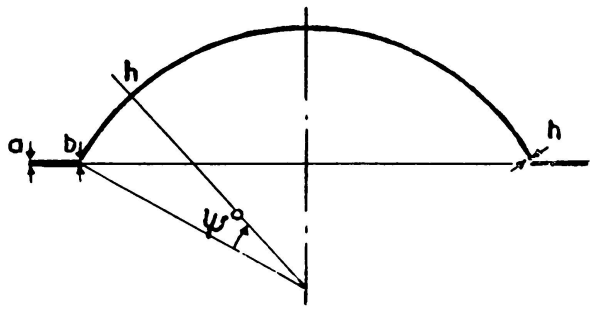

(1/4", 55°)		(1/8", 55°)		(1/16", 55°)		(1/8", 35°)		(1/16", 35°)	
ψ°	h inches	ψ°	h inches	ψ°	h inches	ψ°	h inches	ψ°	h inches
at pt. a	0.250	a	0.125	a	0.065	a	0.125	a	0.065
at pt. b	0.215	b	0.100	b	0.049	b	0.108	b	0.061
0°	0.213	0°	0.100	0°	0.047	0°	0.103	0°	0.053
1°	0.217	1°	0.104	1°	0.048	1°	0.106	1°	0.054
2°	0.213	2.5°	0.106	2.5°	0.051	2.5°	0.108	2.5°	0.055
5°	0.205	5°	0.113	5°	0.054	5°	0.114	5°	0.060
10°	0.213	15°	0.113	15°	0.056	15°	0.120	15°	0.062
15°	0.220	20°	0.117	20°	0.059	20°	0.124	20°	0.065
20°	0.228	25°	0.115	25°	0.060	25°	0.124	25°	0.065
25°	0.233	30°	0.118	30°	0.060	30°	0.125	30°	0.065
30°	0.238	35°	0.121	35°	0.062	35°	0.125	35°	0.065
35°	0.236	40°	0.124	40°	0.064				
40°	0.244	50°	0.125	50°	0.065				
50°	0.248	55°	0.125	55°	0.065				
55°	0.250								

Application of Rim Loading

Rim loading was applied by placing the spherical shells on cast iron rings and applying either vertical loads to produce bending moment or horizontal forces to produce circumferential horizontal forces as shown

diagrammatically in figure 8 and as in the photographs. Two cast iron rings were used, one to fit in with the 55° shell and the other for the 35° shells. It was found out that it was adequate to have 16 equidistant points of loading to produce a fairly uniform load at the shell rim.

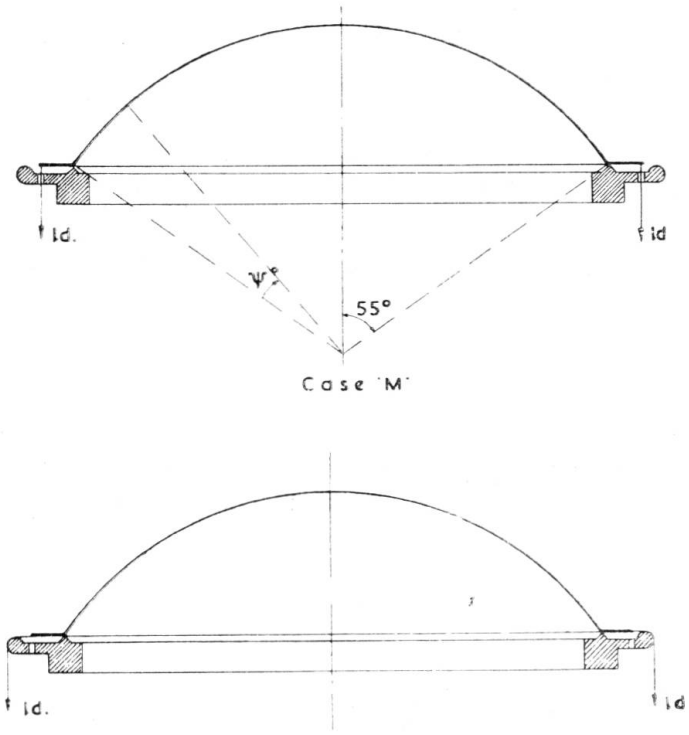

FIG. 8

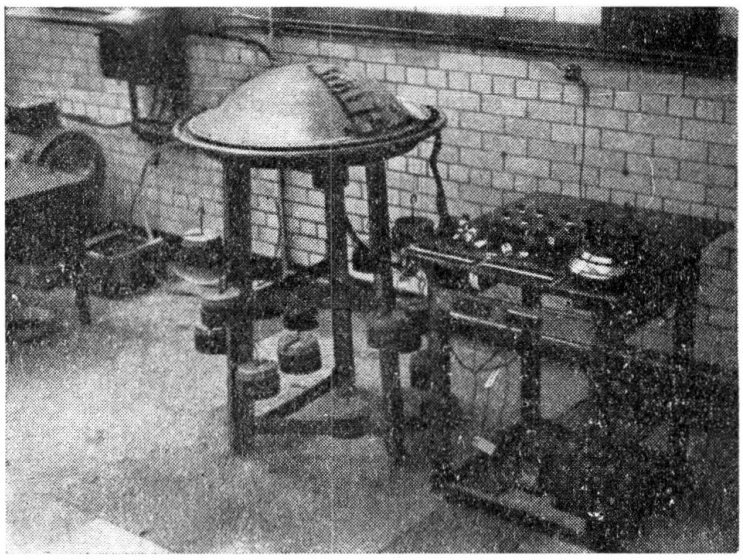

FIG. 9. 55° shells – Case M

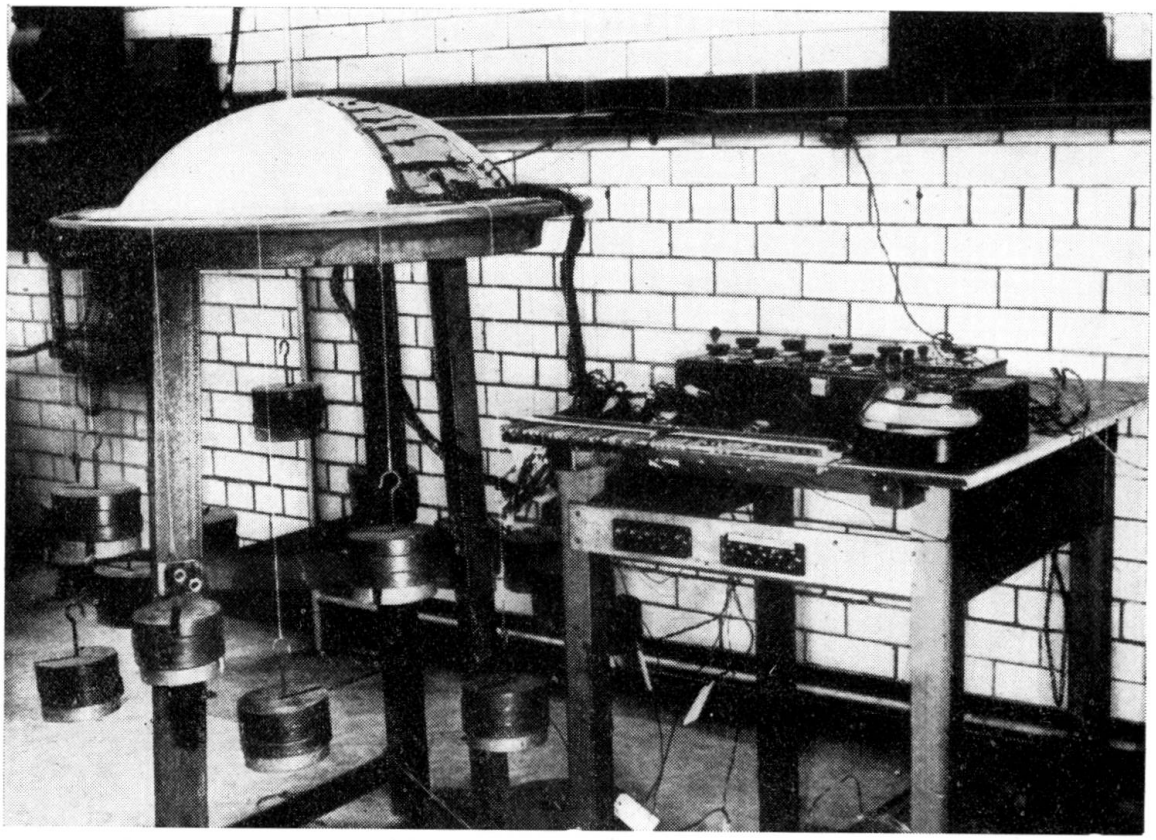

FIG. 10. 55° shells – Case H

FIG. 11. 35° shells – Case H

Procedure of Experiments

The three 55° shells were tested under the condition of continuity of the flange ring. the bending moment test was carried out on the shells and the results presented in figures 13, 14 and 15. The case of the rim bending moment is referred to as «Case M». Although the horizontal force test, which is referred to as «Case H», was carried out on these three shells, yet the readings obtained were so small that no reliable curves could be obtained. The reason was that the test was carried out under the condition of «Flange Ring Continuous» and the force H transmitted to the shell edge was very small as may be seen from equation (5).

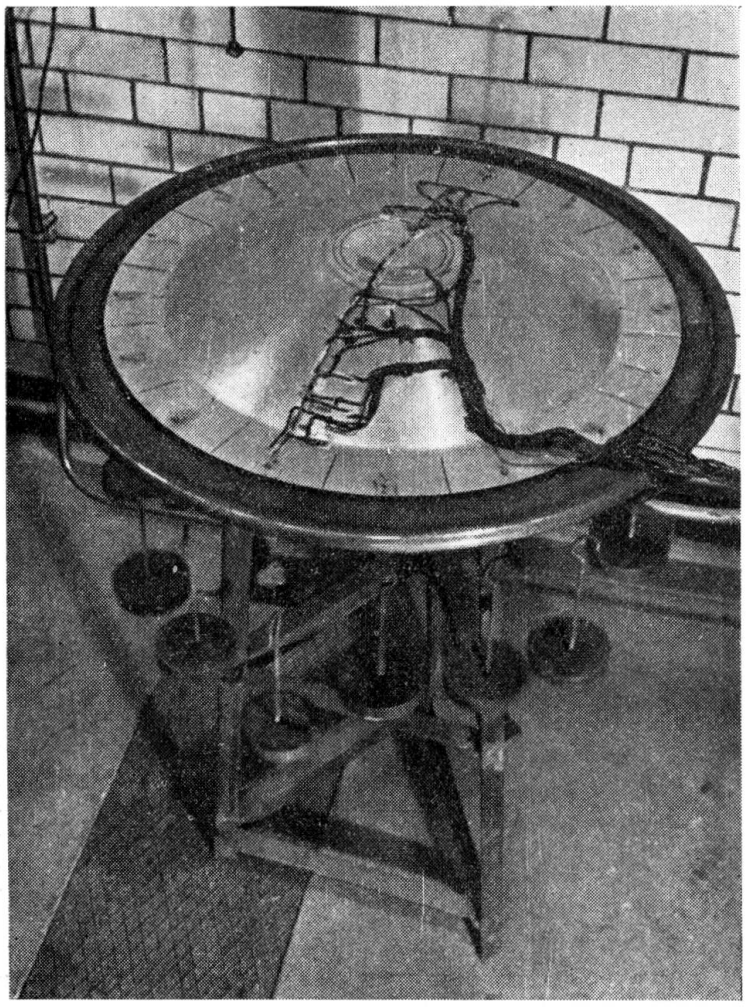

FIG. 12. 35° shell – Case M

The tests for the two 35° shells were therefore carried out for both «Case M» and «Case H» under the two conditions:

1. The flange ring continuous as described for the three 55° shells. For the shell ($^1/_8$", 35°) no appreciable readings could be obtained with the available loadings for Case H, F. Ring Continuous.

2. The flange ring cut at 16 equidistant points between the points of loadings as shown in figure 12. The flange ring was not cut through completely until the shell rim as this might have prevented the use of the same shells for another series of tests not mentioned in this Paper. A distance of $^1/_2$" was left uncut at the edge of the shell. The flange ring after being cut ceased to produce horizontal restraint except that part of the $^1/_2$" ring. The conditions is referred to in figures 16 and 17 for case M and 18 and 19 for case H, as «Experimental F. Ring cut».

Presentation of Results

For all this series of experiments the rim loading was applied in increments and the strains were recorded at the different stations, both when loading and unloading. Knowing the average values of the meridional strain ε_m and the circumferential strain ε_c at any station, the corresponding stresses σ_m and σ_c can be computed by the elastic relations:

$$\sigma_m = \frac{E}{1 - m^2} (\varepsilon_m + m \ \varepsilon_c)$$

$$\sigma_c = \frac{E}{1 - m^2} (\varepsilon_c + m \ \varepsilon_m)$$

For comparison the stresses were calculated for the corresponding value of either $M_\alpha = 1$ lb.in./in. or $H_\alpha = 1$ lb./in. according to the case of loading.

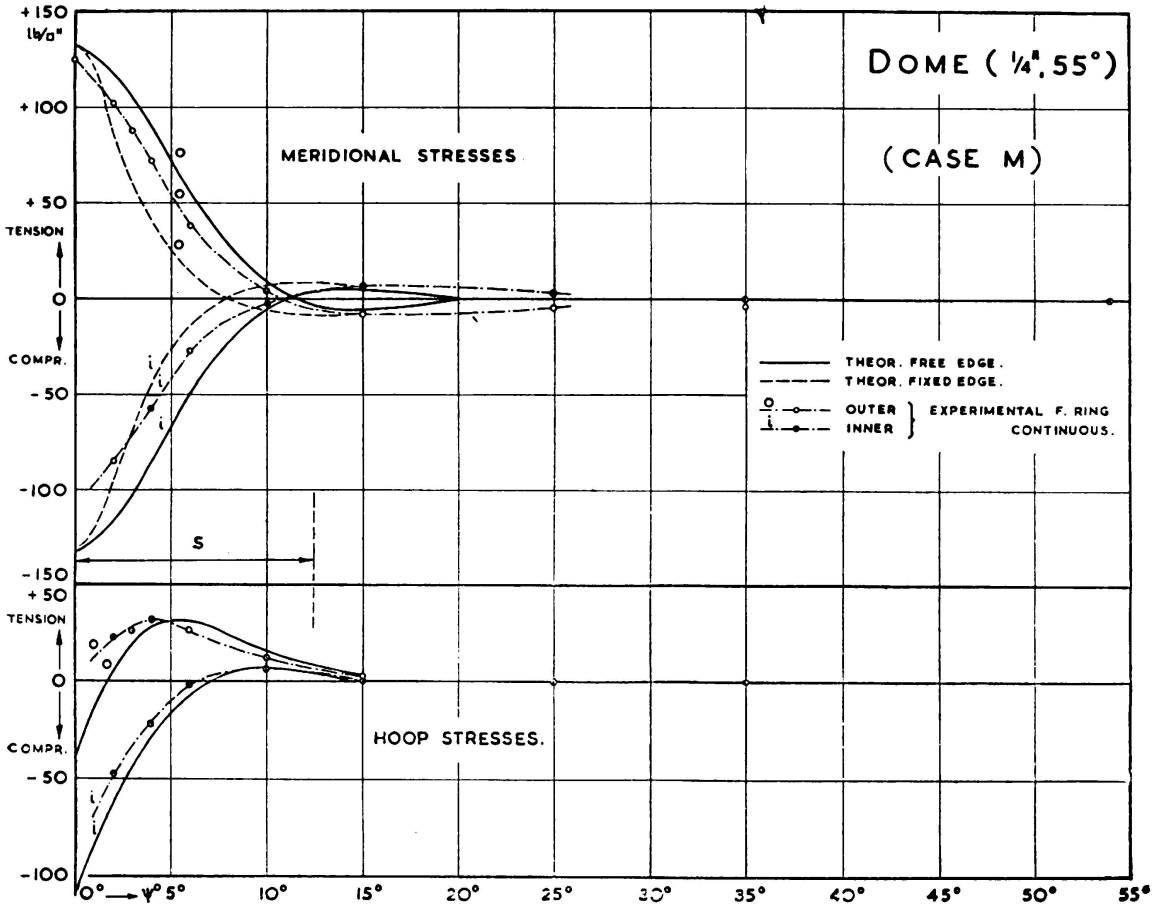

FIG. 13

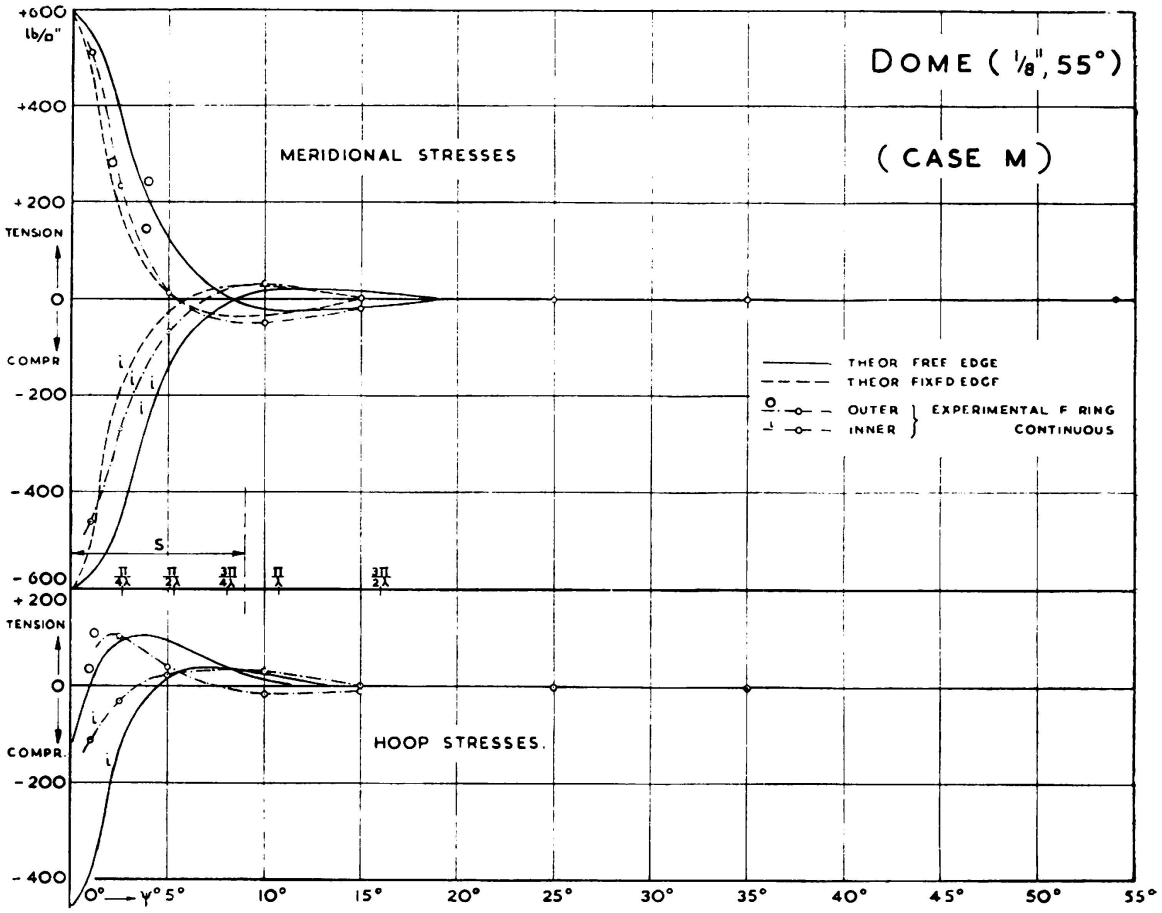
DOME (1/8", 55°)
(CASE M)
MERIDIONAL STRESSES
+600 lb/a"
+400
+200
TENSION
0
COMPR
-200
-400
-600
THEOR FREE EDGE
THEOR FIXED EDGE
OUTER
INNER
EXPERIMENTAL F RING
CONTINUOUS
S
+200
TENSION
0
COMPR.
-200
-400
HOOP STRESSES.
0° ψ° 5° 10° 15° 20° 25° 30° 35° 40° 45° 50° 55°

FIG. 14

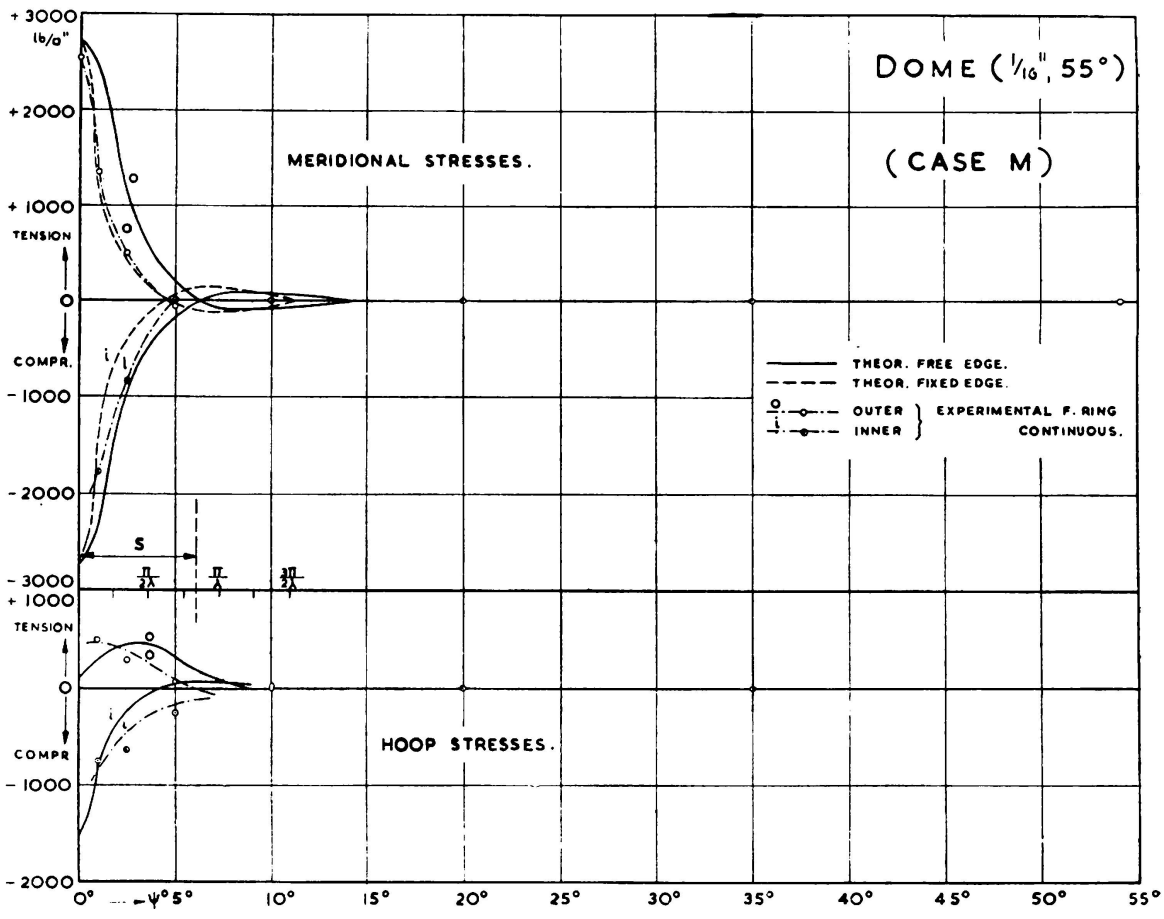
DOME (1/16", 55°)
(CASE M)
MERIDIONAL STRESSES.
+3000 lb/a"
+2000
+1000
TENSION
0
COMPR.
-1000
-2000
-3000
THEOR. FREE EDGE.
THEOR. FIXED EDGE.
OUTER
INNER
EXPERIMENTAL F. RING
CONTINUOUS.
S
+1000
TENSION
0
COMPR
-1000
-2000
HOOP STRESSES.
0° ψ° 5° 10° 15° 20° 25° 30° 35° 40° 45° 50° 55°

FIG. 15

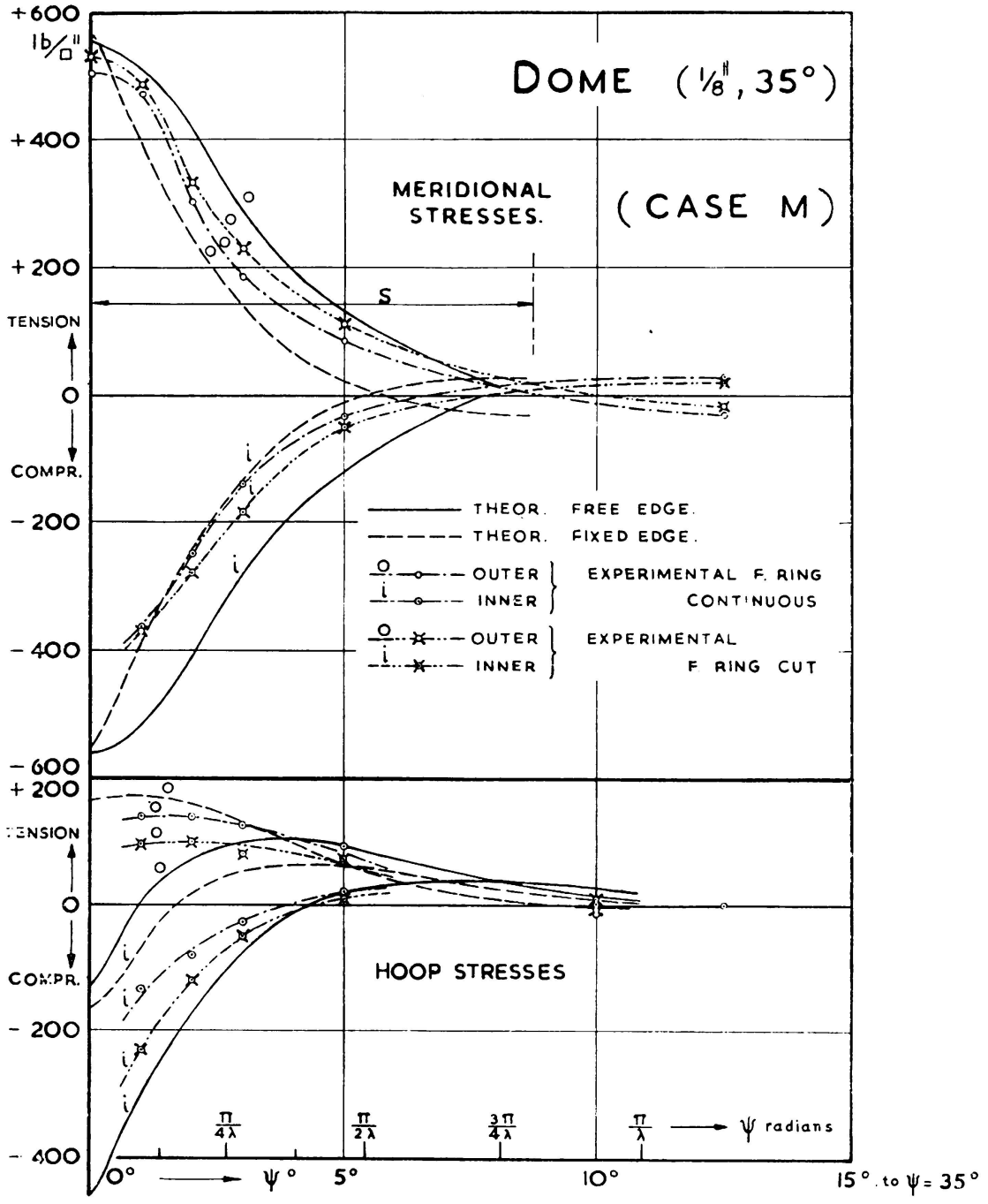

FIG. 16

The experimental stresses are presented on the diagrams, figures 13 to 19 inclusive, together with the stress distribution calculated analytically according to Geckeler's approximate solution as presented in the first part of this Paper. The variation of the thickness of the shells was taken into account. It was found that the stress distribution is very nearly the same for the stresses calculated according to Geckeler's method dealing with the variation of thickness and those calculated according to the simplified method suggested in this Paper as mentioned before.

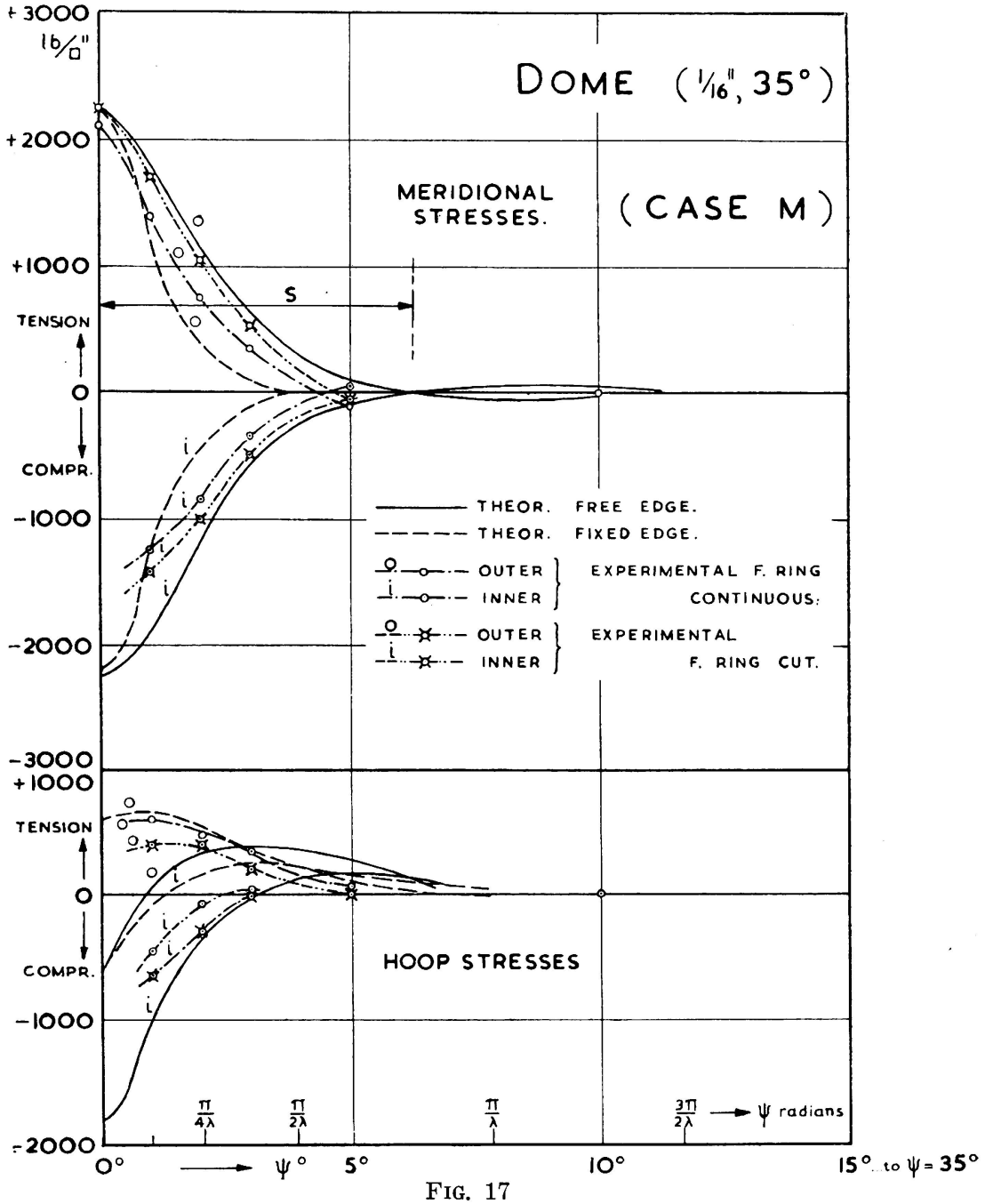

FIG. 17

Discussion of the analytical and experimental distribution of stresses

Studying the distribution of stresses as shown on the diagrams the following points are noted:

1. Both theory and experiment show clearly that the rim loading affects only a limited edge zone. Comparing the diagrams of the shells 35° with those for the shells 55°, it is noticeable that the edge zone is not affected by the angle of opening of the shell (provided that

it is not small). It increases, however, with the increase of thickness of the shell. This rim zone is mainly confined to the distance

$$S = 2\sqrt{ah}$$

2. The meridional stresses obtained from the experiments showed close agreement with the analytical distribution, but with slightly earlier damping. It is, however, recommended that the analytical stress distribution is used for design so as to be on the safe side, since the discrepancy

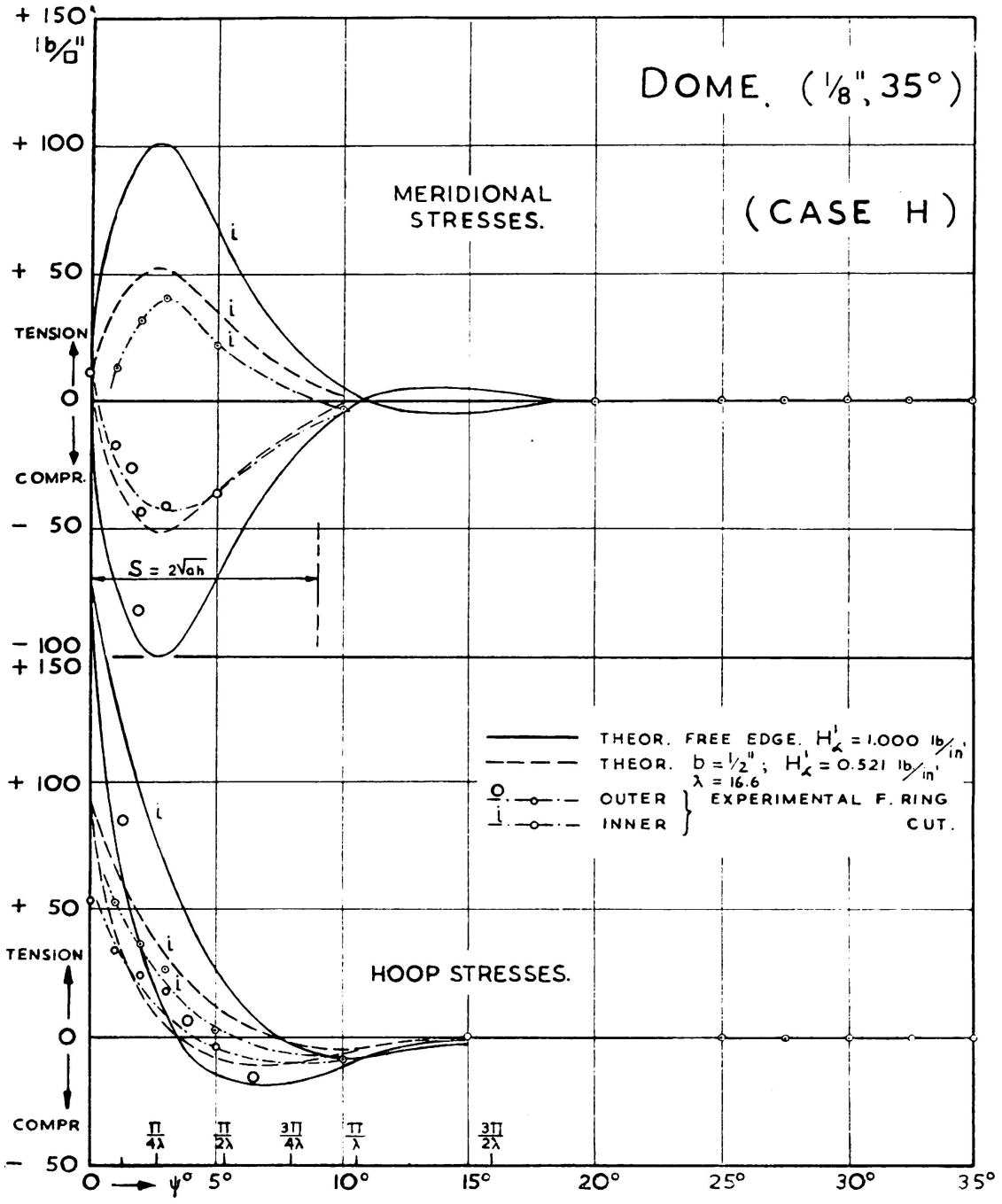

FIG. 18

may be due to the introduction of the fillet between the shell and the flange ring. Nevertheless, it is clear that the stresses due to N_Φ are small compared with those due to M_Φ and therefore N_Φ may be neglected.

3. The experiments showed that the hoop stresses did not have as close agreement to the analytical stresses as the meridional stresses. The reason is probably that the effect of the flange ring is more on N_θ than on M_Φ as may be noticed from equations 2 and 3. In the case of reinforced concrete, however, Poisson's ratio is usually neglected and

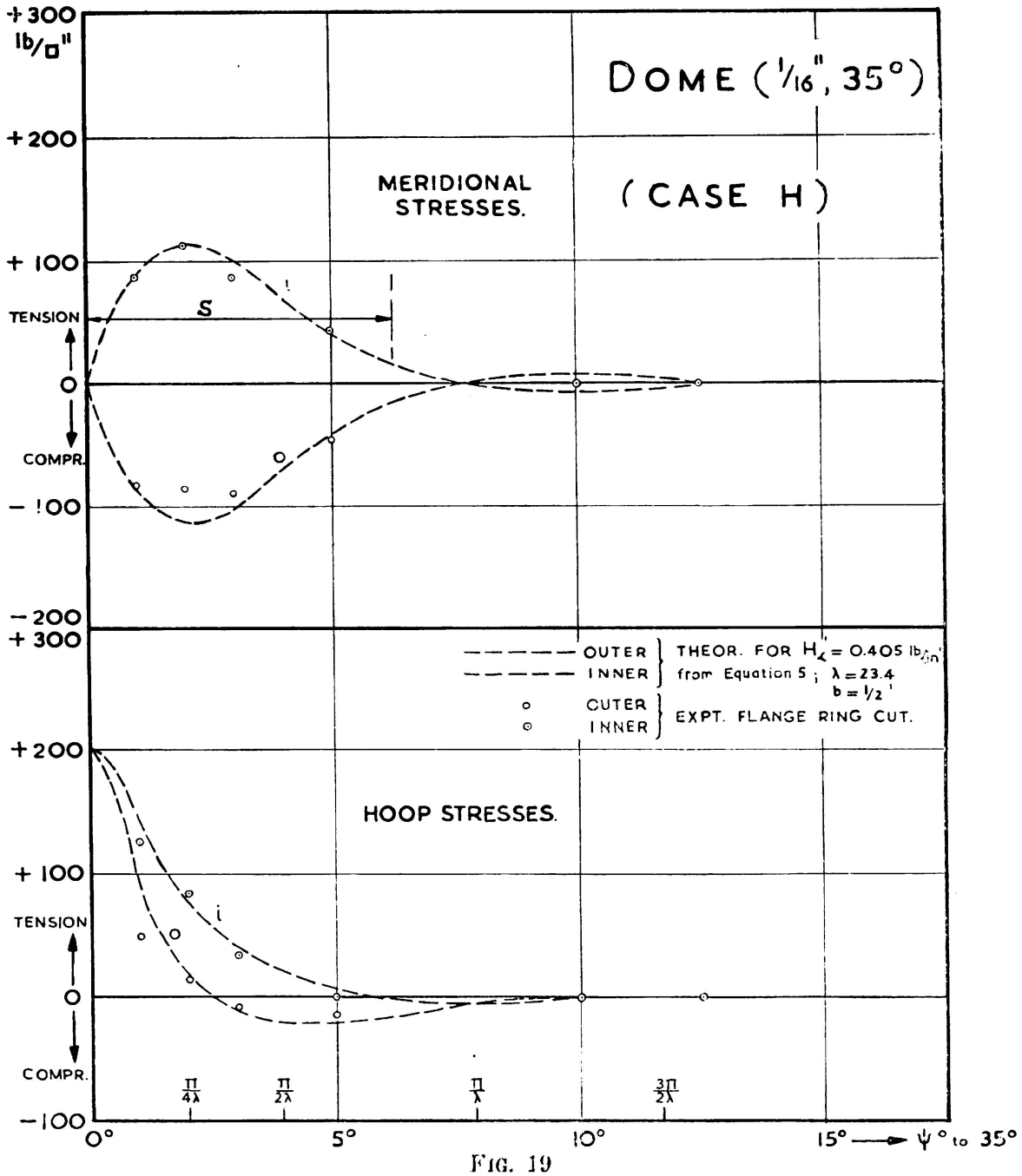

FIG. 19

therefore M_θ can be ignored. In this case the hoop stresses may be calculated from N_θ only.

4. Studying the diagrams for the 35° shells, figures 16, 17, 18 and 19, the effect of cutting the flange ring is noticed. The effect was, however, clearer for Case H than for Case M. The horizontal strain on the edge beam «absorbed» most of the horizontal force H_α according to equation (5).

CONCLUSIONS

A. The theory and experiment showed that:

1. The rim loading affects an edge zone given by $S = 2\sqrt{ah}$, where a is the radius of the spherical shell and h is the thickness.

2. In calculating the stresses in a concrete shell the following equation may apply, based on ignoring the meridional force N_Φ and the circumferential bending moment M_ϑ.

a. for the case of rim bending moment M_α lb. in/in

$$\sigma_m = \pm \frac{6}{h^2} M_\alpha \, e^{-\lambda\psi} (\sin \lambda\psi + \cos \lambda\psi)$$

$$\sigma_c = + \frac{2\lambda^2}{a\,h} M_\alpha \, e^{-\lambda\psi} (\sin \lambda\psi - \cos \lambda\psi)$$

b. for the case of rim horizontal force H_α lb./in.

$$\sigma_m = \pm \frac{6a}{h^2} H_\alpha \sin \alpha \, e^{-\lambda\psi} \sin \lambda\psi$$

$$\sigma_c = + \frac{2}{h} H_\alpha \sin \alpha \, e^{-\lambda\psi} \cos \lambda\psi$$

in which

h is the actual thickness of the point considered
$\lambda = 1.317\sqrt{a/h}$
and α = half the central angle of opening of the shell
and ψ = angle defining the point considered, figure 3.

Instead of calculating the stresses at specific angles ψ, it is easier to calculate these values at $\lambda\psi = 0$, $\frac{\pi}{8}$, $\frac{\pi}{4}$, $\frac{\pi}{2}$ and π using the coefficients given in figure 6.

B. For computing the stress components N_Φ, M_Φ and N_θ for spherical shells with variable thickness, the shell may be considered having a uniform damping factor λ. If the shell is thikened at the edge with a gradual variation of thickness and the thickened part is covering the limit of the edge zone, then an average λ is taken at a distance from rim equal to $0.5\sqrt{a\text{-}h_{av}}$, where h_{av} is the average thickness in the edge zone. The stress components may, then be obtained from the coefficients given in figure 6. Knowing the stress components, the stresses are calculated, but the variation of thickness should be taken into consideration in this case.

BIBLIOGRAPHY

1. GECKELER, J. — «Ueber die Festigkeit Achensymmetrischer Schalen». Forschungsarbeiten auf dem Gebiete des Ingenieurwesens, Heft 276, 1926.
2. HETENYI, M. — «Spherical shells subjected to axial Symmetrical Bending». Publications of International Association for Bridge and Structural Engineering». Zurich, vol. v, 1938.
3. TIMOSHENKO, S. — «Theory of Plates and Shells», McGraw Hill, 1940.
4. HANNA, M. M. — «The Behaviour of thin spherical domes under axisymmetrical loading». Ph. D. Thesis, St. Andrews University, Scotland, 1950.

ACKNOWLEDGMENTS

This paper is a part of a researchwork carried out under the direction of Professor W. T. Marshall, Ph. D., M. I. C. E., M. I. Struct. E., and has been presented for the degree of Ph. D. to St. Andrews University, Scotland.

SUMMARY

The purpose of this Paper is to study experimentally the stress distribution in thin spherical shells when subjected to axisymmetrical bending moment or horizontal force at the rim. Experiments were carried out for these two cases of loading on five aluminium shells having the same radius but different thicknesses or different angles of openings. Strains were measured at near-by and distant stations on the upper and lower surfaces of the shells, by means of electrical wire resistance strain gauges. Stresses were then computed from the experimental strains and compared with the stress distribution obtained from the available theoretical solution.

Both theory and experiment indicate that the rim loading affects only a limited zone near the edge. In this Paper, a simplified formula is presented to define the extent of this rim zone. An easier procedure is also given, by which the stress distribution for these cases of loading may be calculated.

ZUSAMMENFASSUNG

Der Zweck dieser Arbeit liegt darin, auf experimenteller Grundlage die Spannungsverteilung in dünnen Kugelschalen zu bestimmen, die axialsymmetrischen Biegungsmomenten oder Horizontalkräften längs des

Randes unterworfen sind. Diese zwei Belastungsfälle wurden an fünf Aluminiumschalen mit gleichem Radius, aber verschiedener Dicke und verschiedenem Oeffnungswinkel untersucht. Dabei wurde die Beanspruchung an benachbarten und entfernten Stellen, sowohl auf der obern wie der untern Fläche der Schale mit Hilfe von elektrischen Widerstandsmess-Streifen gemessen. Die Spannungen liessen sich aus den gemessenen Dehnungen berechnen, und es folgt ein Vergleich mit der aus der theoretischen Lösung bestimmten Spannungsverteilung.

Sowohl Theorie wie Versuch zeigen, dass die Randbelastung nur eine begrenzte, anliegende Zone beeinflusst. Eine vereinfachte Formel für die Bestimmung der Ausdehnung dieser Randzone kann aus dem vorliegenden Beitrag entnommen werden, ebenso gibt der Verfasser ein einfaches Berechnungsverfahren für die Spannungsverteilung unter diesen Belastungsfällen.

RESUMO

O autor faz um estudo experimental sobre a distribuição das tensões em coberturas delgadas de forma esférica submetidas, ao longo dos bordos, a momentos flectores ou forças horizontais simétricas em relação ao eixo. Fizeram-se ensaios para estes dois casos de carga sobre 5 coberturas de alumínio de raio igual mas de espessura e ângulo de abertura diferentes. Mediram-se as deformações em pontos vizinhos e distantes, nas faces superior e inferior das coberturas, por meio de flexómetros eléctricos de resistência. As tensões foram calculadas a partir das deformações assim determinadas e comparadas com a distribuição de tensões obtida a partir da solução teórica.

Tanto a teoria como os ensaios indicam que a carga periférica influe sòmente sobre uma zona limitada vizinha do bordo. O autor apresenta ainda uma fórmula simplificada que define a referida zona. Também indica um processo simplificado permitindo calcular a distribuição de tensões nestes casos de carga.

RÉSUMÉ

L'auteur décrit une étude expérimentale de la distribution des contraintes dans des voiles minces de forme sphérique soumis, le long de leur bord, à des moments fléchissants, ou des forces horizontales aximétriques. Les essais effectués pour ces deux cas de charge ont porté sur 5 voiles en aluminium de même rayon mais d'épaisseur et angle d'ouverture différents. Les déformations ont été mesurées en des points voisins et distants sur les deux faces des voiles, au moyen de flexomètres à résistance. Les contraintes ont été calculées à partir des déformations ainsi obtenues et comparées à la distribution des contraintes déterminée à partir de la solution théorique.

Tant la théorie que les essais montrent que la charge périphérique n'affecte qu'une zône limitée voisine du bord. L'auteur présente encore une formule simplifiée qui définit cette zône. Il donne également un procédé simplifié permettant de calculer la distribution des contraintes pour ces cas de charge.

Leere Seite
Blank page
Page vide